CrossMark

ORIGINAL PAPER

Hydrothermal Synthesis, Structures and Properties of Two Silver-Containing Organic–Inorganic Hybrids Based on Precursor $[AlW_{12}O_{40}]^{5-}$

Dan-Feng He · Hong-Sheng Liu · Cheng-Gang Ci ·
Zhong-Xin Jin · Ning Li · Hai-Bo Dong ·
Yi-Qing Yu · Chun-Yan Zhang · Mei-Juan Hu

Abstract Two new silver-containing inorganic–organic hybrid compounds [Ag(2-MMIZ)$_2$]$_6$\{[Ag(2-MMIZ)$_2$]$_2$[Ag(2-MMIZ)]$_2$[AlW$_{12}$O$_{40}$]$_2$\} (**1**) and [Ag(2-MMIZ)$_2$]$_5$ [AlW$_{12}$O$_{40}$] (**2**) based on Keggin polyoxometalates and Ag complex have been successfully synthesized by reaction of AgNO$_3$, 2-MMIZ (2-methylimidazole), and the α-Na$_5$[AlW$_{12}$O$_{40}$]·13H$_2$O precursor under hydrothermal conditions, and these two compounds were well characterized by elemental analyses, IR spectrum, UV–Vis spectrum, Thermogravimetric analyses, Powder X-ray diffraction measurements and single-crystal X-ray diffraction. The structure of Compound **1** represents the first dimer anion \{[Ag(2-MMIZ)$_2$]$_2$[Ag(2-MMIZ)]$_2$[AlW$_{12}$O$_{40}$]$_2$\}$^{6-}$ and six free [Ag(2-MMIZ2]$^+$ segments as cations, among the five crystallographically independent of [Ag(2-MMIZ)] segments in **1**, Ag atoms exist three types of coordination configurations including linear, triangular and T type. Compound **2** is composed of one α-Keggin polyoxoanion [AlW$_{12}$O$_{40}$]$^{5-}$ and five free [Ag(2-MMIZ)$_2$]$^+$ segments as cations, there is only a linear coordination mode of Ag atoms in **2**. Compounds **1** and **2** show photocatalytic activity for degradation of organic dye Rhodamine-B.
Graphical Abstract The first dimmer anion \{[Ag(2-MMIZ)$_2$]$_2$[Ag(2-MMIZ)]$_2$ [AlW$_{12}$O$_{40}$]$_2$\}$^{6-}$ based on [Ag(2-MMIZ)]$^+$ cations, [Ag(2-MMIZ)$_2$]$^+$ cations and [AlW$_{12}$O$_{40}$]$^{5-}$ polyoxoanions can be used for degradation of organic dye Rhodamine-B.
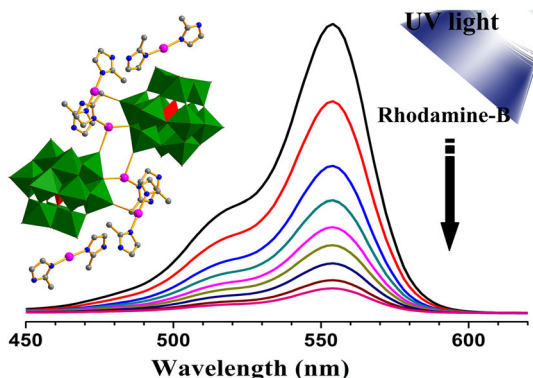
D.-F. He · H.-S. Liu (✉) · C.-G. Ci · Z.-X. Jin · N. Li · H.-B. Dong · Y.-Q. Yu ·
C.-Y. Zhang · M.-J. Hu
School of Chemistry and Chemical Engineering, Key Laboratory of Oilfield Applied Chemistry,
Daqing Normal University, Daqing 163712, Heilongjiang, People's Republic of China
e-mail: hsliu899@126.com

 Springer

Introduction

Polyoxometalates (POMs), discrete anionic transition-metal oxide clusters, are remarkable for their molecular and electronic structural diversity [1, 2]. They have received considerable current interest because of their wide range of physical and chemical properties and their significant applications in many fields including catalysis, medicine, magnetism, and materials science [3–5]. Therefore, POMs can be used as available and controllable secondary building units (SBUs) to construct POM-based inorganic–organic hybrid compounds with specific properties and functions [6]. Up to now, a number of POM-based inorganic–organic hybrid compounds have been synthesized and characterized [7, 8].

α-Na$_5$[AlW$_{12}$O$_{40}$]·13H$_2$O was synthesized according to the method reported by Weinstock et al. [9]. α-Na$_5$[AlW$_{12}$O$_{40}$]·13H$_2$O can be used as a precursor for the new inorganic–organic hybrid materials, but it is quite dynamic and unstable when the pH value varies. Both the pH value and temperature need to be controlled cautiously during the synthesis. To the best of our knowledge, there are no literatures on synthesis of POM-based inorganic–organic hybrid compounds by employing AlW$_{12}$O$_{40}$ precursor and single ligand, even to obtain two compounds with analogous structures through subtle adjusting of reaction conditions.

As a d^{10} transition-metal, the Ag(I) possesses high affinity for O and N donors, various coordination numbers of two to seven in covalent complexes, and versatile geometries [10–12]. These features enable Ag(I) to be frequently used as a metallic linker and a good candidate in constructing organic–inorganic hybrid compounds. Moreover, silver-containing compounds are actively involved components of ultraviolet (UV-) and visible-light photocatalysts for pollutant degradation [13], H$_2$ evolution [14], and water oxidation [15]. With the incorporation of conventional POMs and silver-containing materials, the silver-POMs have showed promising function in recent years [16–25]. However, it continues to be a meaningful work to

expand the hybrid compounds based on the silver coordination compounds and POM clusters for their potential as photocatalyst.

In this work, by employing $\alpha\text{-Na}_5[\text{AlW}_{12}\text{O}_{40}]\cdot13\text{H}_2\text{O}$, 2-Methylimidazole and AgNO_3, two organic–inorganic hybrids formulated as $[\text{Ag}(2\text{-MMIZ})_2]_6\{[\text{Ag}(2\text{-MMIZ})_2]_2[\text{Ag}(2\text{-MMIZ})]_2[\text{AlW}_{12}\text{O}_{40}]_2\}$ (**1**) and $[\text{Ag}(2\text{-MMIZ})_2]_5[\text{AlW}_{12}\text{O}_{40}]$ (**2**) were synthesized under hydrothermal conditions, and both of them have good reproducibility and high purity. The two compounds showed good catalytic activity for photodegradation of rhodamine-B(RhB) under UV light irradiation.

Experimental Section

Materials and Methods

All reagents were readily available from commercial sources and used as received without further purification. The IR spectra in KBr pellets were recorded in the range 400–4,000 cm^{-1} with an Alpha Centaurt FT/IR spectrophotometer. Powder X-ray diffraction (XRD) measurements were performed on a Rigaku D/MAX-3 instrument with Cu Kα radiation in the angular range $2\theta = 3°-60°$ at 293 K. Elemental analysis C, H and N were determined on a Perkin-Elmer 2400 CHN elemental analyzer. Thermogravimetric analyses were carried out by using a Perkin-Elmer TGA7 instrument, with a heating rate of 10 °C/min, under a nitrogen atmosphere.

Synthesis of Compound $[Ag(2\text{-}MMIZ)_2]_6\{[Ag(2\text{-}MMIZ)_2]_2[Ag(2\text{-}MMIZ)]_2[AlW_{12}O_{40}]_2\}$ (1)

$\alpha\text{-Na}_5[\text{AlW}_{12}\text{O}_{40}]\cdot13\text{H}_2\text{O}$ (0.41 g, 0.127 mmol) was dissolved in 5 mL water, and then a solution (5 mL) containing AgNO_3 (0.14 g, 0.63 mmol) and 2-Methylimidazole (0.11 g, 1.3 mmol) was added dropwise. The pH was ultimately adjusted to 5.1–5.3. The resulting mixture was stirred for 1 h and then transferred to an 18 mL Teflon-lined reactor, kept at 140 °C for 3 days, and then cooled to room temperature. Brown block crystals were obtained by filtering, washed with distilled water and dried in air (yield: 41 %). IR (KBr disks): 1622(w), 1565(w), 1424(w), 1351(w), 1275(vw), 1100(w), 952(s), 882(s), 800(s), 762(s), and 538(w). Elemental anal. Calcd for **1** (%): C, 10.42; H, 1.31; N, 6.07. Found: C, 10.35; H, 1.33; N, 5.99.

Synthesis of Compound $[Ag(2\text{-}MMIZ)_2]_5[AlW_{12}O_{40}]$ (2)

Compound **2** was synthesized analogously to compound **1** except that the pH was finally adjusted to 3.3-3.5 and the reaction temperature was 100 °C. Brown sheet crystals were obtained by filtering, washed with distilled water and dried in air (yield: 53 %). IR (KBr disks): 1622(w), 1566(w), 1429(w), 1280(vw), 1159(w), 1101(w), 951(s), 881(s), 803(vs), 764(s), and 531(w) cm^{-1}. Elemental anal. Calcd for **2**: C, 11.33; H, 1.24; N, 6.60. Found: C, 11.25; H, 1.21; N, 6.71.

X-ray Crystallography

Single-crystal diffractometry was conducted on a Bruker Smart Apex CCD diffractometer with Mo Kα monochromated radiation ($\lambda = 0.71073$ Å) at room temperature. The linear absorption coefficients, scattering factors for the atoms, and anomalous dispersion corrections were taken from the international tables for X-ray crystallography [26]. Empirical absorption corrections were applied. The structures were solved by using the direct method and refined through the fullmatrix least-squares method on F^2 using SHELXS-97 [27]. Anisotropic thermal parameters were used to refine all non-hydrogen atoms, with the exception for some oxygen atoms. Crystallization water molecules were estimated by thermogravimetry and only partial oxygen atoms of water molecules were achieved with the X-ray structure analysis. The crystal data and structure refinement results of **1** and **2** are summarized in Table 1. CCDC reference nos. are 911022 and 911023 for **1** and **2**, respectively. These data can be obtained free of charge from The Cambridge Crystallographic Data Centre via www.ccdc.cam.ac.uk/data_request/cif.

Table 1 Crystal data and structural refinement for compounds **1** and **2**

Formula	**1** $C_{72}H_{144}Ag_{10}Al_2N_{36}O_{80}W_{24}$	**2** $C_{40}H_{52}Ag_5AlN_{20}O_{41}W_{12}$
Formula weight (gmol^{-1})	8,338.9	4,241.4
T (K)	296 (2)	296 (2)
Wavelength (Å)	0.71073	0.71073
Crystal system	Triclinic	Triclinic
Space group	P-1	P-1
a (Å)	13.838 (3)	12.570 (3)
b (Å)	13.870 (3)	13.472 (3)
c (Å)	20.725 (4)	14.123 (3)
α (°)	86.56 (3)	66.73 (3)
β (°)	86.85 (3)	64.66 (3)
γ (°)	68.68 (3)	77.32 (3)
V (Å^3)	3,696.6 (13)	1,982.1 (7)
Z	1	1
D_{calc} (mg m^{-3})	3.730	3.554
μ (mm^{-1})	19.982	18.644
F (000)	3,704	3,432
Crystal size (mm)	0.21 × 0.21 × 0.13	0.25 × 0.24 × 0.22
Goodness-of-fit on F^2	1.047	1.085
Final R indices [I > 2σ(I)]	R$_1^a$ = 0.0603, wR$_2^a$ = 0.1261	R$_1^a$ = 0.0828, wR$_2^a$ = 0.1757
R indices (all data)	R$_1^a$ = 0.0920, wR$_2^a$ = 0.1393	R$_1^a$ = 0.0931, wR$_2^a$ = 0.1816

^{a} $R_1 = \sum ||F_o| - |F_c|| / \sum |F_o|$, $wR_2 = \left\{ \sum \left[w(F_0^2 - F_c^2)^2 \right] / \sum \left[w(F_o^2)^2 \right] \right\}^{1/2}$

Photocatalytic Experiments

The photocatalytic experiments of **1** and **2** for the photodegradation of RhB under UV irradiation have been checked through a typical process: before the photocatalytic experiment, 150 mg of the compounds with water stability were dispersed into 100 mL of 10.0 mg L^{-1} RhB solution in a beaker and the mixture was stirred for 1 h. When the surface-adsorption on the powders of **1** and **2** reached to equilibrium, the mixture was stirred continuously under UV irradiation from a 125 W high pressure Hg lamp with a distance of 4.3 cm between the liquid surface and the lamp. Every 30 min, 4.0 mL of the sample was taken out from the beaker, followed by removal of the compound particles with centrifugation, and the clear solution was monitored by UV–Vis spectroscopy.

Results and Discussion

Synthesis and Structure

Compounds **1** and **2** were obtained under hydrothermal conditions as shown in "Experimental Section" section. Multiple parallel experiments indicated that compound **1** was synthesized at higher pH and temperature. This may be due to the raw materials are more readily to form polymers under the above condition. To the best of our knowledge, **1** and **2** were the first examples of analogues that prepared from single ligand and the Keggin [AlW$_{12}$O$_{40}$]$^{5-}$ precursor through subtle adjusting of reaction conditions.
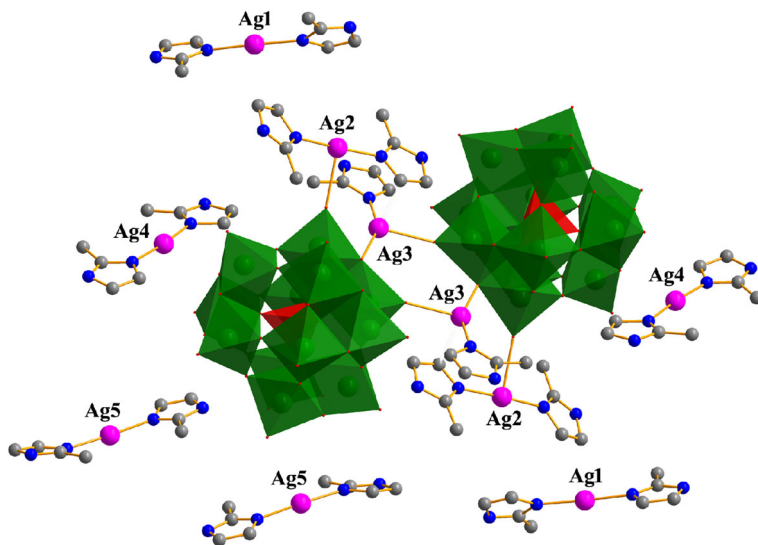
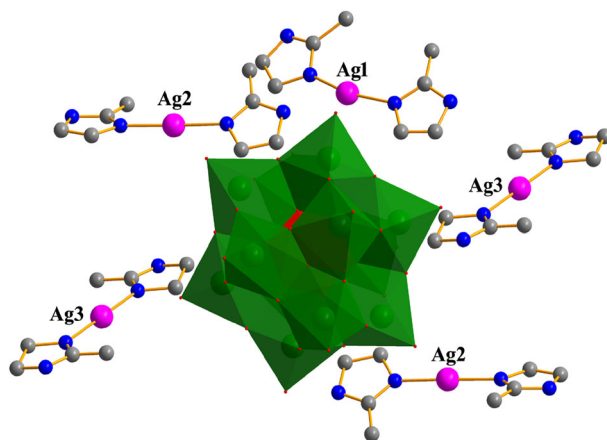**Fig. 1** Combined polyhedral/ball-and-stick representation of **1**. Color scheme for polyhedra: WO6 (*green*), AlO4 (*red*); for balls: Ag (*pink*), N (*blue*), and C (*grey*) (Color figure online)

Compound **1** was composed of six $[Ag(2\text{-MMIZ})_2]^+$ cations and one $\{[Ag(2\text{-}$ $MMIZ)_2]_2[Ag(2\text{-MMIZ})]_2[AlW_{12}O_{40}]_2\}^{6-}$ dimer anion. The dimer anion is composed of two $[Ag(2\text{-MMIZ})]^+$ cations, two $[Ag(2\text{-MMIZ})_2]^+$ cations and two $[AlW_{12}O_{40}]^{5-}$ polyoxoanions, as shown in Fig. 1. The dimmic Keggin derivatives have been widely formed in the monolacunary, dilacunary, and trilacunary POMs, but they were less observed in saturated POMs. There are strong π–π stacking interactions between the counteractions and the adjacent segments. The $[Ag(2\text{-}$ $MMIZ)_2]$ in **1** are cis–trans isomerism owing to the different location of the methyl-groups. $[Ag4(2\text{-MMIZ})_2]$ and $[Ag5(2\text{-MMIZ})_2]$ segments are cis-form and $Ag2(2\text{-}$ $MMIZ)_2$ segments are trans-form. 2-MMIZs in $[Ag1(2\text{-MMIZ})_2]$ are not exactly in the same plane, the dihedral angle of two 2-MMIZ is 46.3°. Ignoring the cis–trans isomerism of $[Ag(2\text{-MMIZ})_2]^+$, there are three types of coordination configurations for the five crystallographically independent of $[Ag(2\text{-MMIZ})]$ segments in **1**, as shown in Fig. 2. (1) Ag1 and Ag5 acting as free cations are similar to that in **2**, showing linear coordination mode by coordinating with two nitrogen atoms from two 2-MMIZ ligands. (2) Ag3 adopts a distorted triangular coordination model and coordinates to an N atom from 2-MMIZ ligand (with Ag–N distance of 2.13 Å) as shown in Table S1; simultaneously, it coordinates to an Ob atom and an Od atom from two adjacent $[AlW_{12}O_{40}]^{5-}$ units resulting in the dimer [28]. The Ag–Ob bond lengths are 2.57 Å and the Ag–Od distance is 2.26 Å. The N–Ag3–O bond angles and O–Ag3–O bond angles are in the range of 92.5° to 150.5°. (3) Acting as hanging segments, Ag2 and Ag4 adopt three coordination T type models. Ag2 links to two 2-MMIZ ligands with N–Ag2–N bong angle of 176.1° and one Od atom form $[AlW_{12}O_{40}]^{5-}$ units with Ag2–Od distance of 2.60 Å. Ag4 links to two 2-MMIZ ligands with N–Ag4–N bong angle of 176.1° and one Od atom form $[AlW_{12}O_{40}]^{5-}$ units with Ag4–Ob distance of 2.81 Å.

The structure of compound **2** is composed of one α-Keggin polyoxoanion $[AlW_{12}O_{40}]^{5-}$ and five free $[Ag(2\text{-MMIZ})_2]^+$ segments as cations, as shown in Fig. 3. All the Ag atoms are dicoordination, and adopt a linear coordination mode by coordinating with two nitrogen atoms from two 2-MMIZ ligands. The Ag–N distances in **2** are in the range of 2.27(2)–2.373(18) Å, and the N–Ag–N bong
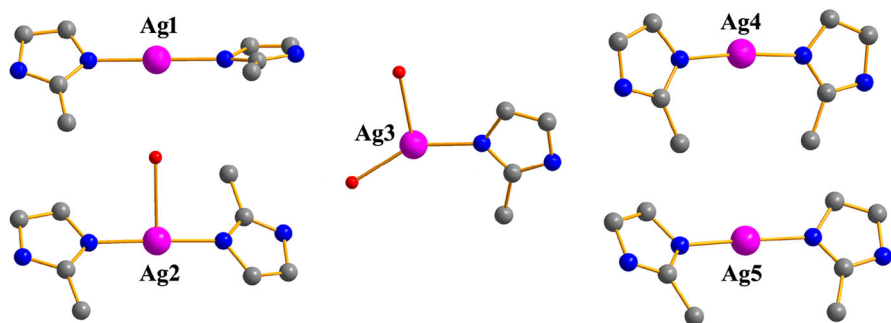
Fig. 2 Coordination configurations for five crystallographically independents of [Ag(2-MMIZ)] segments in **1**

Fig. 3 Combined polyhedral/ball-and-stick representation of **2**. Color scheme for polyhedra: WO6 (*green*), AlO4 (*red*); for balls: Ag (*pink*), N (*blue*), and C (*grey*) (Color figure online)

angles are in the range of 165° to 180°, as shown in Table S2. The [Ag(2-MMIZ)$_2$] are cis–trans isomerism in **2**, [Ag1(2-MMIZ)$_2$] segments are cis-form and Ag3(2-MMIZ)$_2$ segments are trans-form. 2-MMIZs in [Ag2(2-MMIZ)$_2$] are not exactly in the same plane, the dihedral angle of two 2-MMIZ is 33.7°.

Bond valence sums (BVS) analysis based on the observed bond lengths for **1** and **2** suggests the formal valences of W^{6+}, Ag$^+$ and Al^{3+} [29–31]. The BVS value of the O atoms in **1** and **2** are between 1.75 and 2.07, indicating all O are noprotonated. The amount of counter cations in **1** and **2** are respectively coincident with the negative charge of anions.

FT-IR Spectroscopy

As shown in Figure S1, the IR spectra of **1** and **2** display similar characteristic vibration patterns derived from the Keggin-type precursor in the low-wavenumber region (<1,000 cm^{-1}), namely, v_{as}(W–O$_d$), v_{as}(Al–Oa), v_{as}(W–Ob), and v_{as}(W–Oc). These characteristic vibration bands appear at 952(s), 882(s), 800(s), and 762(s) for **1**, 951(s), 881(s), 803(s), and 764(s) cm^{-1} for **2**. Comparing with **2**, there are slight shifts for vibrational stretches of W–Od and W–Ob in the IR spectrum of **1**, demonstrating strong binding interactions between Keggin unit and [Ag(2-MMIZ)] segments in **1**. Bands in regions of 1,620 and 1,073 cm^{-1} are characteristics of 2-MMIZ ligands [32].

Powder X-ray Diffraction Patterns and Thermogravimetric Curves

The experimental powder X-ray diffraction (PXRD) patterns of **1** and **2** are in good agreement with the simulated patterns, which indicate the phase purity of the samples, as shown in Figures S2 and S3. The thermal behaviors of compounds **1** and **2** have been studied by means of thermogravimetric (TG) measurements as shown

in Figure S4. The TG curves of compounds **1** and **2** exhibit one step of weight loss. In the temperature range of 30–600 °C, the weight loss of **1** is 82.91 % (calcd. 83.12 %) and the weight loss of **2** is 83.93 % (calcd. 83.44 %) corresponding to the collapse of the framework and the release of the decomposition of organic ligands in them.
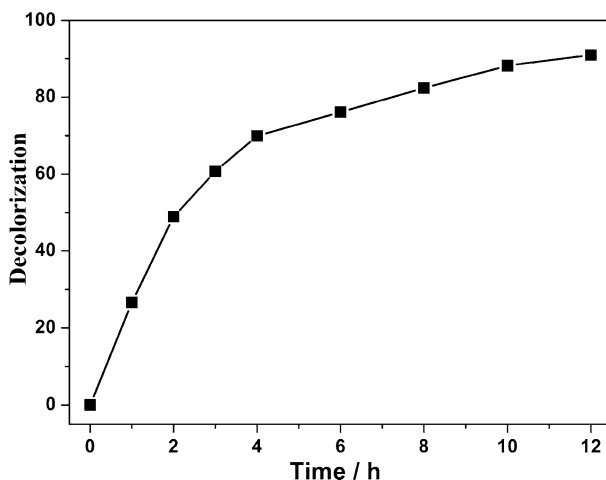
Photocatalytic Activity

It is known that POMs often show photocatalytic activity in the degradation of some organic substances under UV irradiation [33]. In the UV–Vis absorption spectra as shown in Figure S5, there is an absorption band in the visible region, which represents the photocatalytic activity of compounds **1** and **2**. The photocatalytic activity of compounds **1** and **2** were tested by degradation of organic dye Rhodamine-B (RhB, 10 mg L^{-1}) solutions. As shown in Fig. 4, under UV light irradiation, **1** exhibits fast and effective degradation of RhB, and detailed experiment processes are shown in the "Experimental Section" section. The characteristic absorbance of RhB decreased with the increasing time of visible light irradiation at 554 nm. The relative absorbance of RhB (A/A_0, where A_0 is the initial absorbency of the RhB solution corresponding to the maximum absorption peak; A is the absorbency of RhB solution after UV light irradiation at a time) versus reaction time (t) is shown in figures. The conversion of RhB can be expressed by the following equation: $[(A_0-A)/A_0] \times 100 \%$. As shown in Fig. 5, the decoloration of RhB reached to 90.9 % after twelve hours of UV light irradiation. However, compound **2** did not display fast degradation of RhB compared with **1**, as shown in
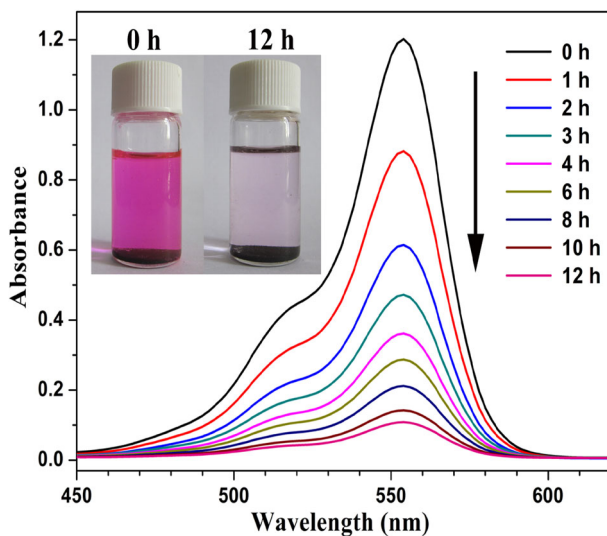
Fig. 4 UV–Vis spectra changes of the RhB solutions as a function of irradiation time in the presence of compounds **1**. Initial concentrations: RhB (10 mg L^{-1}, pH ∼2.5); **1** (150 mg L^{-1}). Photographs of **1** for photocatalysis reaction: before (*left*) and after (*right*) photocatalysis reaction

Fig. 5 Decolorization rates of RhB in the presence of compound **1**

Figure S6. After four runs of photocatalytic tests, the catalytic activity of **2** did not display significant loss when RhB was re-added to the system. Twelve hours later, the absorbance of the RhB is about 48.1 % of the original solution. In addition, $Na_5[AlW_{12}O_{40}] \cdot 13H_2O$ are added in the RhB solutions instead of compounds **1** and **2** for contrast, as shown in Figure S7 and S8: it exhibited weak photocatalytic activity in the degradation of RhB under UV irradiation. The experiments results indicate that the photocatalytic activity of compounds **1** and **2** not only stems from the $[AlW_{12}O_{40}]^{5-}$ component, but also comes from the [Ag(2-MMIZ)]. The powder XRD patterns of compounds **1** and **2** after the photocatalytic reaction remain unchanged compared with the as prepared sample, which suggests the compounds **1** and **2** might be the potential photocatalyst with photocatalytic activity in the degradation of some organic dyes.

Conclusions

In conclusion, two silver-containing inorganic–organic hybrid compounds based on Keggin-type polyoxoanion $[AlW_{12}O_{40}]^{5-}$ were successfully synthesized under hydrothermal conditions. Compound **1** is composed of six $[Ag(2-MMIZ)_2]^+$ cations and one $\{[Ag(2-MMIZ)_2]_2[Ag(2-MMIZ)]_2[AlW_{12}O_{40}]_2\}^{6-}$ dimer anion. Compound **2** is composed of five free $[Ag(2-MMIZ)_2]^+$ segments as cations and one α-Keggin polyoxoanion $[AlW_{12}O_{40}]^{5-}$. Photocatalytic analysis indicates that compounds **1** and **2** showed good catalytic activity for photodegradation of rhodamine-B(RhB) under UV light irradiation. The exploration of Ag-based inorganic–organic hybrid POMs with high-dimension is underway.

References

1. M. T. Pope *Heteropoly and Isopoly Oxometalates* (Springer, Berlin, 1983).
2. M. T. Pope and A. Müller (1991). *Angew. Chem. Int. Ed.* **30**, 34.
3. N. Mizuno and M. Misono (1998). *Chem. Rev.* **98**, 199.
4. J. T. Rhule, C. L. Hill, and D. A. Judd (1998). *Chem. Rev.* **98**, 327.
5. E. Coronado and C. J. Gómez-García (1998). *Chem. Rev.* **98**, 273.
6. P. Gouzerh and A. Proust (1998). *Chem. Rev.* **98**, 77.
7. J. Zhang, J. Hao, Y. G. Wei, F. P. Xiao, P. C. Yin, and L. S. Wang (2010). *J. Am. Chem. Soc.* **132**, 14.
8. E. F. Wilson, H. N. Miras, M. H. Rosnes, and L. Cronin (2011). *Angew. Chem. Int. Ed.* **50**, 3720.
9. I. A. Weinstock, J. J. Cowan, Elena M. G. Barbuzzi, H. D. Zeng and C. L. Hill (1999). *J. Chem. Soc.* **121**, 4608.
10. J. Q. Sha, J. Peng, Y. Q. Lan, Z. M. Su, H. J. Pang, A. X. Tian, P. P. Zhang, and M. Zhu (2008). *Inorg. Chem.* **47**, 5145.
11. H. I. S. Nogueira, F. A. AlmeidaPaz, P. A. F. Teixeira, and J. Klinowski (2006). *J. Chem. Commun.* **28**, 2953.
12. H. J. Pang, J. Peng, J. Q. Sha, A. X. Tian, P. P. Zhang, Y. Chen, and M. Zhu (2009). *Mol. Struct.* **921**, 289.
13. M. Zhu, P. Chen, and M. Liu (2011). *ACS Nano.* **5**, 4529.
14. S. J. Li, S. M. Liu, S. X. Liu, Y. W. Liu, Q. Tang, Z. Shi, S. X. Ouyang, and J. H. Ye (2012). *J. Am. Chem. Soc.* **134**, 19716.
15. N. Kakuta, N. Goto, H. Ohkita, and T. Mizushima (1999). *J. Phys. Chem. B.* **103**, 5917.
16. G. C. Lica, K. P. Browne, and Y. Y. Tong (2006). *J. Chem. Soc.* **17**, 349.
17. R. J. Liu, S. W. Li, X. L. Yu, G. J. Zhang, Y. Ma, and J. N. Yao (2011). *J. Mater. Chem.* **21**, 14917.
18. T. McGlone, C. Streb, M. B. Fité, J. Yan, D. Gabb, D. L. Long, and L. Cronin (2011). *Cryst. Growth Des.* **11**, 2471.
19. C. Streb, C. Ritchie, D. L. Long, P. Kgerler, and L. Cronin (2007). *Angew. Chem. Int. Ed.* **119**, 7723.
20. G. G. Gao, P. S. Cheng, and T. C. W. Mak (2009). *J. Am. Chem. Soc.* **51**, 18257.
21. C. Streb, R. Tsunashima, D. A. MacLaren, T. McGlone, T. Akutagawa, T. Nakamura, A. Scandurra, B. Pignataro, N. Gadegaard, and L. Cronin (2009). *Angew. Chem. Int. Ed.* **48**, 490.
22. Y. Kikukawa, Y. Kuroda, K. Yamaguchi, and N. Mizuno (2012). *Angew. Chem. Int. Ed.* **51**, 2434.
23. X. L. Zhao and T. C. W. Mak (2010). *Inorg. Chem.* **49**, 3676.
24. D. B. Dang, Y. N. Zheng, Y. Bai, X. Y. Guo, P. T. Ma, and J. Y. Niu (2012). *Cryst. Growth.* **12**, 385.
25. G. Y. Luan, Y. G. Li, S. T. Wang, E. B. Wang, Z. B. Han, C. W. Hu, N. H. Hu, and H. Q. Jia (2003). *Dalton Trans.* 233. doi:10.1039/B208531C.
26. N. F. M. Henry and K. Lonsdale (eds.) *International Tables for X-ray Crystallography* (Kynoch Press, Birmingham, 1952).
27. G. M. Sheldrick *SHELXS-97: Programs for Crystal Structure Solution* (University of Göttingen, Göttingen, 1997).
28. Oa is the oxygen atom bond to the Al atom, Ob is the bridging oxygen atom shared by two W atoms from different W_3O_{13} clusters, Oc is the bridging oxygen atom shared by two W atoms from the same W_3O_{13} cluster, and Od is the terminal oxygen atom combined with only one W atom.
29. I. D. Brown and D. Altermatt (1985). *Acta Crystallogr. Sect. B.* **41**, 244.
30. S. T. Zheng, J. Zhang, J. M. C. Juan, D. Q. Yuan, and G. Y. Yang (2009). *Angew. Chem. Int. Ed.* **48**, 7176.
31. B. Gordin, J. Vaissermann, P. Herson, L. Ruhlmann, M. Verdaguer and P. Gouzerh (2005). *Chem. Commun.* 5624. doi:10.1039/B510434C.
32. L. Han, P. P. Zhang, H. S. Liu, H. J. Pang, Y. Chen, and J. Peng (2010). *J. Chem. Soc.* **21**, 81.
33. P. P. Zhang, J. Peng, H. J. Pang, J. Q. Sha, M. Zhu, D. D. Wang, M. G. Liu, and Z. M. Su (2011). *Cryst. Growth Des.* **11**, 2736.